Electromagnetic Realization of Orders-of-Magnitude Tunneling Enhancement in a Double Well System

Ilya Vorobeichik,* Edvardas Narevicius, Gershon Rosenblum, Meir Orenstein,† and Nimrod Moiseyev‡
OpTun Ltd., MTM Scientific Industries Center, Building 22, P.O. Box 15017, Haifa 31905, Israel
(Received 1 July 2002; published 2 May 2003)

We report on tunneling enhancement in a periodically perturbed double well system. The double well system was realized by a structure of two optical waveguides. The transfer of light power from one waveguide to the another as induced by the periodic variations of the waveguide geometry was investigated. Our experimental measurements show that, in the presence of periodic perturbation, this transfer of light power can be enhanced by more than 500 times. We use an analogy between electromagnetic wave optics and the quantum wave phenomena to provide an experimental support to the theoretical model of tunneling enhancement of a quantum particle, facilitated by its interaction with auxiliary quantum states.

DOI: 10.1103/PhysRevLett.90.176806 PACS numbers: 73.40.Gk, 03.65.Ta, 42.25.–p, 42.50.Hz

Two novel phenomena have been discovered in the theoretical studies of tunneling in a symmetric double well potential perturbed by a monochromatic driving field: the enhancement of tunneling between two potential wells [1–8] and the coherent suppression of tunneling [9–12]. The first phenomenon has been called "the chaos assisted tunneling." The rationale behind this name is that, for sufficiently strong driving, the classical phase space of the driven double well problem consists of a pair of symmetric regular "islands" near the minima of the unperturbed potential, embedded in a bound chaotic "sea." The chaos assisted tunneling mechanism has been shown to be associated with a transition through an intermediate state, which for a sufficiently strong driving is a chaotic one [4–6]. However, it has been shown in Refs. [8,13] that the tunneling enhancement can also be obtained in a weakly driven system, such that all the states involved in the tunneling enhancement phenomenon are regular. This regime is the subject of this report.

In our experiments, the double well system was realized by the transfer of light power between two parallel optical waveguides. We use the analogy between the classical (Maxwellian) wave optics and the quantum wave phenomena. It is known that one can migrate theories and scenarios from the field of classical electromagnetism and quantum mechanics with mutual benefit to both fields.

In weakly guiding dielectric structures, the electric field satisfies the paraxial wave equation [14]:

$$\left[-\frac{\hbar_e^2}{2}\nabla_{x,y}^2 + V(x,y,z)\right]\Psi = i\hbar_e\frac{\partial\Psi}{\partial z}, \tag{1}$$

where

$$V(x,y,z) = \frac{1}{2}\left[1 - \left(\frac{n(x,y,z)}{n_0}\right)^2\right], \tag{2}$$

$n(x,y,z)$ and n_0 are, respectively, the index of refraction at the waveguide core and the waveguide cladding, $\hbar_e = \lambda/(2\pi n_0)$, and λ is the free space wavelength. The scalar electric field (which stands for the nonzero component of a linearly polarized vector electric field) is related to the solution of Eq. (1) through $E(x,y,z) = e^{ik_0 z}\Psi(x,y,z)$, where $k_0 = (2\pi/\lambda)n_0$ and $\Psi(x,y,z)$ varies slowly along the propagation axis, z. The paraxial wave Eq. (1) is an exact mathematical analogue of the time-dependent Schrödinger equation, with $V(x,y,z)$ playing the role of the potential energy term and the propagation axis, z, playing the role of time.

The experimental setup is schematically described in Fig. 1. The optical waveguides were fabricated using planar silica over silicon technology. The waveguides' core was made from a silica oxinitride glass, embedded in a silica glass with a lower refractive index. The waveguide structure consisted of two coupled optical waveguides as shown in Fig. 1. The light was injected into the chip by illuminating the input facet of the chip. The light emerging from the exit facet was monitored.

We have used a highly monochromatic linearly polarized light from a tunable laser at a wavelength of 1550 nm, coupled to a polarization maintaining fiber in order to choose a horizontal linear polarization of the light. The input fiber had a 10 μm in diameter spot size, and it was placed at a distance of 10 μm from the chip facet. By a proper spatial coupling (changing the location of the input fiber), we were able to excite almost exclusively either the ground (localized) mode or a high (extended) mode of the structure. The exit facet was imaged using a long working distance objective $\times 50$ or $\times 100$ onto an infrared camera. This allowed us to obtain submicron resolution of the facet light intensity distribution that corresponded to the predicted spatial power distribution of the modes.

In our experiments, three different cases were considered. In the first, the refractive index of the waveguide core n was uniform along the propagation axis, z, and the structure was multimode over the whole structure length. In the second, symmetric periodic variations

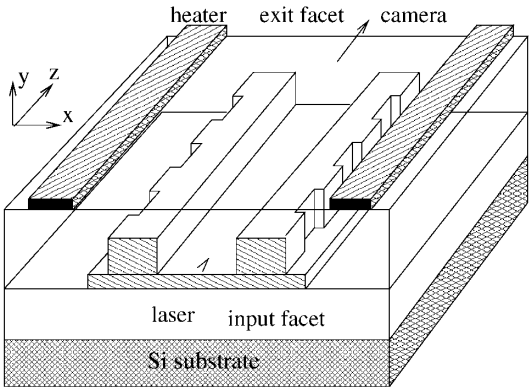

FIG. 1. The schematics of the optical chip with imposed periodic variations of the waveguide width and heaters placed on top of the chip. The dark area stands for the waveguide core embedded in the cladding. The refractive index of the core is $n(x, y) = n_1 = 1.485$, and the refractive index of the cladding is $n_0 = 1.445$. The waveguide width is 7 μm and the distance between waveguides is 15 μm. The thickness of the thin optical layer between waveguides is 0.6 μm and the total waveguides' thickness is 2.5 μm. The total length of the waveguide structure is 11 mm and the length of the periodic structure is 7 mm. The input/output regions consisted of two parts: a uniform waveguide structure of two isolated single-mode waveguides (length of 1 mm) and a tapering to a multimode structure with a length of an additional 1 mm.

of the waveguide geometry were imposed on both waveguides. The periodic structure was generated by changing the width of the parallel waveguides in a periodic fashion (as shown in Fig. 1). In addition, the waveguides were fabricated in a way that the waveguide structure on the input and on the output facets did not support the intermediate high-order modes localized in between the waveguides. It was achieved by gradually tapering the structure to become two isolated single-mode waveguides at the input/output facets. This modification allowed us to avoid the excitation of high-order modes due to incorrect input fiber positioning and to increase the measurement accuracy. In the third case, the periodic variations were imposed only on one of the waveguides, whereas the second one remained uniform and the single-mode waveguide tapering was introduced only close to the input facet. In the output facet region, the waveguide structure was the same multimode structure as in the uniform waveguide experiments. This allowed us to detect the excitation of high-order modes localized in between the waveguides.

The analogue to the two almost degenerate bound quantum states, which are exponentially localized inside the two potential wells, are the two trapped optical modes, which are associated with almost degenerate propagation constants. The waveguide structure was designed such that the first two pairs of trapped modes are localized inside each one of the two waveguides. The second trapped mode of the first pair has a nearly identical intensity distribution as the first mode, but has a different symmetry; i.e., its field amplitude is antisymmetric with respect to the center of the structure. Because of the different symmetry of the first two modes, a linear combination of these modes provides a wave packet which is localized either in the left or in the right waveguide. The waveguide parameters were designed such that the studied optical waveguide structure also supported three optical modes localized in between the waveguides. We will show later that the modes localized in between the waveguides (or above "the potential barrier") play a fundamental role in the tunneling enhancement mechanism.

The first series of experiments was performed on a uniform waveguide structure in order to identify the modes of the unperturbed structure and to measure the unperturbed tunneling rate. To measure the tunneling rate experimentally, the incoming light beam was directed into the left waveguide and the two almost degenerate trapped modes were excited. In Fig. 2(a), we show a photograph of the exit facet of the device, when the incoming light beam has been directed into the left waveguide. As one can see from our measurement, the light beam is localized in the left waveguide and the transfer of light power to the right waveguide is very small. We collected the light from both waveguides and measured the power ratio by a power meter with dynamic range of 10^9. This measurement showed that the power ratio between the left and the right waveguide is slightly larger than 1000. The theoretically predicted value for the power ratio is 10^5. The 2 orders of magnitude difference between the theoretically predicted ratio results from a background noise of the measurement due to the imperfect coupling of the laser light to one of the waveguides

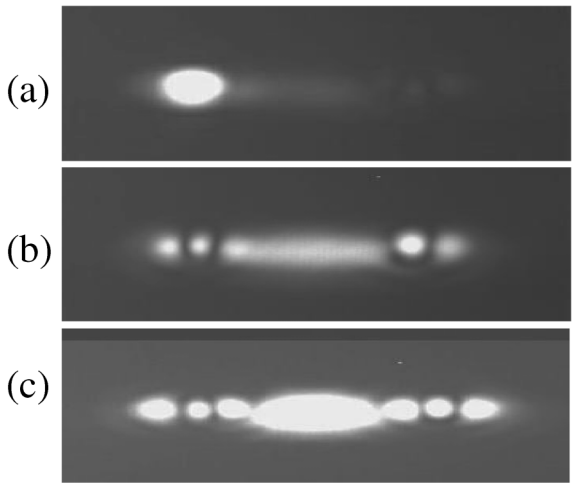

FIG. 2. A picture taken by a camera on the exit facet of the two unperturbed waveguides. The incoming light beam has been directed into the chip and the position of the incoming light was varied such that different modes were preferentially excited: (a) the first almost degenerate pair of trapped optical modes; (b) the fourth-order mode; (c) the sixth-order mode.

and from manufacturing errors. In order to measure the nodal structure of the optical modes that are not localized in the wells separated by a barrier, the incoming light beam has been inserted in between the two separated waveguides (i.e., at the effective "potential" barrier). By doing that, we were able to excite high-order modes which are not localized only in the separate waveguides, but are modes that are spread over the whole waveguide structure (intermediate modes). By changing the position of the fiber, we were able to preferentially excite symmetric modes localized between the waveguides. The optical modes of fourth order and of sixth order are shown in Figs. 2(b) and 2(c), respectively.

The results of the first series of experiments performed on the unperturbed waveguide structure have confirmed that in our experiment the effective potential barrier is too large to allow a significant "tunneling" of light from one waveguide to another within a propagation distance which is shorter than the length of our device. In addition, the presence of high-order modes localized between the waveguides was demonstrated. The modal fields of the modes were in qualitative agreement with the theoretical calculations performed for the studied waveguide structure.

To experimentally investigate the tunneling enhancement by means of periodic perturbation and to prove the effect of the contribution of the auxiliary states, we performed the measurements of optical power transfer in the presence of periodic structure. The waveguide structures were manufactured with periodic variations of the waveguide width along the light propagation axis (grating) shown in Fig. 1. The waveguide width was periodically reduced along the propagation axis. Different periods of variation were considered, keeping the amplitude of the variation constant. In addition, the refractive index of the structure was changed dynamically by heating the structure uniformly along the propagation axis (Fig. 1). Because of the thermo-optic effect, the refractive index of silica is temperature dependent, such that $\Delta n = (dn/dT)\Delta T$, with $(dn/dT) \simeq 1.15 \times 10^{-5}\ \mathrm{K}^{-1}$.

In this second set of experiments, we measured the tunneling rate for different periods of the perturbation (from 80 to 120 μm with a step of 5 μm) and for different temperatures of both heaters. These grating periods were chosen according to the theoretical estimation of resonant coupling between the first mode and the auxiliary modes localized above the barrier. Large variation of periods was also used to compensate for manufacturing errors. In addition, single-mode input and output regions were used to avoid the sensitivity to the initial fiber positioning illustrated in the first series of experiments. All the measurements for a perturbation with a period different from 80 μm shared a common feature; namely, no significant tunneling enhancement has been observed independent of the heaters' temperature (up to 150 °C above ambient temperature). However, for the period of 80 μm, the amount of power transferred from the left waveguide to the right waveguide depended strongly on the heater temperature. For a particular heater temperature difference, a significant tunneling enhancement occurred, and an almost total light power transfer to the right waveguide was measured as shown in Fig. 3(a). For another heater temperature difference, a tunneling rate was reduced significantly, and most of the light power remained in the left waveguide as shown in Fig. 3(b). By comparing the power transferred to the right waveguide in the perturbed case with the power remained in the left waveguide in the unperturbed case, we obtained that slightly more than 50% of the power was transferred. The power that remained in the left waveguide was less than 1% of the initial power. The rest of the signal was lost due to the incomplete power transfer from the intermediate modes to the localized modes. Because of the tapering to a structure of two isolated single-mode waveguides close to the output facet, the optical power carried by the intermediate modes was coupled to the radiative optical modes and did not reach the detector. Some of the remaining power could still be seen in between the waveguides in Fig. 3. In the measurement of the unperturbed waveguides, the power in the right waveguide was more than 1000 times smaller than the power in the left waveguide. Therefore, the experiment shows 500 times enhancement of the tunneling rate. Note that the correct evaluation of the power transfer is possible only when having two isolated single-mode waveguides at the output, since the excited intermediate modes (carrying 50% of the total power) would otherwise smear out completely the output intensity distribution.

The thermo-optic effect induces a change in the level spacing between the fundamental mode and the

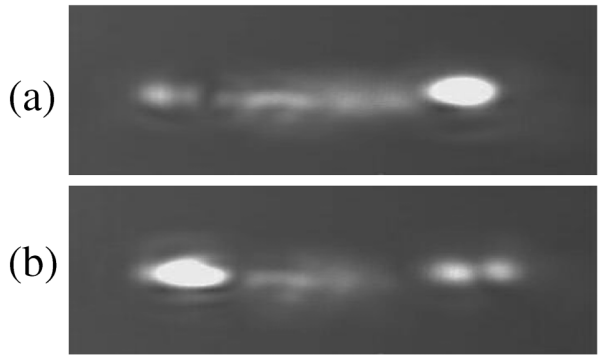

FIG. 3. A picture taken by a camera on the exit facet of the waveguides when the incoming light beam has been directed into the left waveguide and the periodic variation of the geometry of both waveguides were applied. The amplitude of the waveguide width variations is equal to 0.5 μm and the period is equal to 80 μm. (a) The left heater is not heated and the right heater is heated by 150 °C. A significant light power transfer to the right waveguide is obtained. (b) The left heater is heated to 40 °C and the right heater is not heated. The light power transfer to the right waveguide is suppressed.

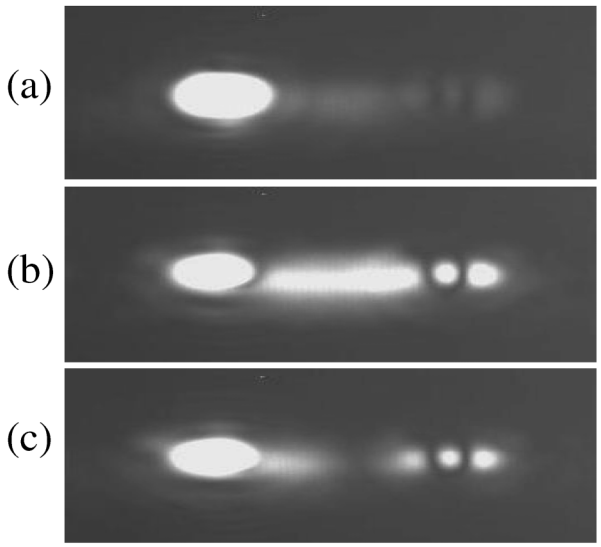

FIG. 4. A picture taken by a camera on the exit facet of the waveguides when the incoming light beam has been directed into the left waveguide and the periodic variation of the geometry of the left waveguide were applied. The waveguide variation parameters are the same as in Fig. 3. The right heater was not heated. (a) The left heater temperature is 6 °C. Most of the light remains in the left waveguide. (b) The left heater temperature is 95 °C. The fourth-order mode [Fig. 2(b)] is partially excited. (c) The left heater temperature is 79 °C. The linear combination of the fifth- and the sixth-order modes is excited.

ntermediate modes. Consequently, the applied heating results in a mismatch between the level spacing and the static perturbation period. Therefore, the change in the tunneling rate due to the heating demonstrates strong dependence of the tunneling on the level spacing between the ground state and the extended states above the barrier. The sensitivity of the tunneling rate to the period of the perturbation and to the detuning induced by heating shows that the enhancement of tunneling is due to the coupling between the ground state and the auxiliary states.

To prove the importance of the intermediate modes to the tunneling enhancement, we performed the second type of dynamic measurements (involving heating). We repeated the measurements of power transfer from the left waveguide to the right waveguide but, in this case, the static perturbation was applied to the left waveguide only. The right waveguide remained uniform. In addition, since the single-mode tapering was not introduced in the output facet region, we could detect directly the excitation of high-order modes localized in between the waveguides.

The results of the experiments with one-sided grating were similar to the results of the two-sided grating experiments. For a perturbation period different from 80 μm, no significant power transfer from the left waveguide has been observed independent of the heaters' temperature. However, for the period of 80 μm, excitation of intermediate modes has been detected. Again, in this case, the excitation depended strongly on the heaters' temperature. For all temperatures a linear combination of intermediate modes has been excited. By changing the temperature difference between two heaters we were able to change the amount of power transferred to a particular intermediate mode as shown in Fig. 4.

This set of experiments shows that the intermediate modes localized between the potential wells are excited for the perturbation parameters for which the tunneling enhancement has been obtained. Therefore, this illustrates the fact that the enhancement of tunneling is due to the coupling between the ground state and the intermediate states.

To the best of our knowledge, this is the first experiment that demonstrated the enhancement of tunneling through a potential barrier by several orders of magnitude by means of periodic perturbation. We have shown that, in our studied case, the tunneling enhancement is due to the interaction between the ground state and the additional auxiliary states of the double well system.

We thank Mr. Anatoly Meller for his help in optical measurements.

*Email address: ilya.vorobeichik@optun.com
†Permanent address: Department of Electrical Engineering, Technion-Israel Institute of Technology, Haifa 32000, Israel.
‡Permanent address: Department of Chemistry and Minerva Center for Nonlinear Physics, Technion-Israel Institute of Technology, Haifa 32000, Israel.
Email address: nimrod@tx.technion.ac.il

[1] W. A. Lin and L. E. Ballentine, Phys. Rev. Lett. **65**, 2927 (1990).
[2] A. Peres, Phys. Rev. Lett. **67**, 158 (1991).
[3] J. Plata and J. M. Gomez-Liorente, J. Phys. A **25**, L303 (1992).
[4] R. Utermann, T. Dittrich, and P. Hanggi, Phys. Rev. E **49**, 273 (1994).
[5] O. Bohigas, S. Tomsovich, and D. Ullmo, Phys. Rep. **223**, 43 (1993).
[6] S. Tomsovich and D. Ullmo, Phys. Rev. E **49**, 273 (1994).
[7] M. Holthaus, Phys. Rev. Lett. **69**, 1596 (1992).
[8] I. Vorobeichik and N. Moiseyev, Phys. Rev. A, **59**, 2511 (1999).
[9] F. Grossmann, T. Dittrich, P. Jung, and P. Hanggi, Phys. Rev. Lett. **67**, 516 (1991); Z. Phys. B **84**, 315 (1991).
[10] F. Grossmann and P. Hanggi, Europhys. Lett. **18**, 571 (1992).
[11] R. Bavli and H. Metiu, Phys. Rev. Lett. **69**, 1986 (1992).
[12] M. Steinberg and U. Peskin, J. Appl. Phys. **85**, 270 (1999).
[13] I. Vorobeichik, M. Orenstein, and N. Moiseyev, IEEE J. Quantum Electron. **34**, 1772 (1998).
[14] K. Kawano and T. Kitoh, *Introduction to Optical Waveguide Analysis: Solving Maxwell's Equations and the Schrödinger Equation* (Wiley-Interscience, New York, 2001).